

Trading off robustness and performance in receding horizon control with uncertain energy resources

Mahraz Amini

Mads Almassalkhi

Department of Electrical and Biomedical Engineering, University of Vermont, Burlington, USA
{mamini2,malmassa}@uvm.edu

Abstract—Increased utilization of residential and small commercial distributed energy resources (DERs) has led DER aggregators to develop concepts such as the virtual power plants (VPP). VPPs aggregate the energy resources and dispatch them akin to a conventional power plant or grid-scale battery to provide flexibility to the system operator. Since the level of flexibility from aggregated DERs is uncertain and time varying, the VPPs’ dispatch can be challenging. To improve the system operation, flexible VPPs can be formulated probabilistically and can be realized with chance-constrained model predictive control (CCMPC). This can be solved using scenario-based methodology, which provides a-priori probabilistic guarantees on constraint satisfaction. This paper focuses on understanding the robustness and performance trade offs in receding horizon control with uncertain energy resources. The CCMPC dispatches robustly the uncertain VPPs and conventional generators while taking into account economically optimal, secure reference trajectory for generating assets. Closed-loop performance is with respect to minimizing the deviation of conventional generators from their reference trajectory. To evaluate the trade off between robustness and system performance with uncertain energy resources, a simulation-based analysis is carried out on the modified IEEE 30-bus system.

Index Terms—model predictive control, energy storage, robust optimization, uncertainty, dynamic capacity saturation, chance constrained.

I. INTRODUCTION

In recent years, environmental and energy concerns have led to increased penetration of distributed energy resources (DERs), such as solar photovoltaic and wind generation, which represents both a challenge and opportunity for grid operators. The intermittency of renewable energy sources as well as forecast uncertainties in load, price, and renewable in-feed profiles, call for storage solutions and appropriate control strategies [1]. So far, imbalances between production and load are compensated by fast acting reserves from generators, such as gas turbines or hydro storage power plants. However, due to the on-going increase in intermittent sources, day-ahead planning becomes more demanding. Independent System Operators (ISOs) can pay high penalties when load forecasts are inaccurate and require generators re-scheduling to balance demand and supply [2]. Furthermore, an increasing number of backup generation units is needed, running on reduced power or even idling, to quickly react to output changes of intermittent sources. Instead of compensating forecast uncertainties with fast acting backup generators, as it is often done

in practice, the imbalances can also be compensated by means of coordinating flexible energy resources, i.e., demand dispatch [3], [4].

Recently, the concept of Virtual Power Plants (VPPs) has been proposed as a novel technology for aggregating and coordinating a large fleet of residential flexible energy resources, including electric battery storage, thermostatically controlled loads (TCLs), and deferrable loads. The VPP offers the aggregate flexibility to the system operator as a synthetic reserve to preserve grid stability [5]. When called upon, the VPP can rapidly respond to changes in net-load by quickly coordinating its fleet of assets to provide requested balancing reserves [6]. Since offered flexibility by VPPs to the system operator is limited, to benefit the most from them, careful planning through smart techniques such as MPC is required.

Today, in practice, based on market conditions and load and renewable forecasts, an optimal power flow problem is solved with a day ahead window prediction horizon (i.e. 24 hours) on an hour by hour time scale to provide an economically optimal schedule for generators and flexible resources [7]. However, due to variable uncertainty in the net-load forecast, there will always be mismatches between scheduled operating set-points and the actual operating points. Therefore, the scheduled operating point may no longer be feasible and balancing reserves are required and can be provided by a set of VPPs by adjusting the aggregate output of DERs [8].

As a VPP derives its flexibility from aggregating thousands of DERs, estimation of the VPP’s current energy state, energy limits, and up/down power capabilities are inherently uncertain and time-varying. Therefore, this paper seeks to formulate the VPP’s flexibility in a probabilistic manner with chance constraints. Then, we solve this by a scenario-based approach, which provides a-priori guarantee to the probabilistic constraints [9], [10]. The authors in [9], [11] use probabilistically robust optimization method provides a priori guarantees on the probability of constraint violation without needing any knowledge of the uncertainty distribution, however it requires large number of uncertainty scenarios. Other recent studies also solve chance constraint problem using scenario approach as authors do in [12], or by using analytical reformulation, e.g., [13], but these studies do not model the uncertainty on the VPP’s capacity.

To take uncertainty of VPP’s energy capacity into account, we employ chance constraints to a receding-horizon model predictive controller (MPC) that is similar to the author’s prior work in [14], [15]. At each step, net-load forecasts (i.e., load minus renewable generation) and dynamic states (e.g., storage and generators) are updated to provide a prediction of

This work was supported by the U.S. Department of Energys Advanced Research Projects Agency - Energy (ARPA-E) award DE-AR0000694.

power imbalances. The chance-constrained predictive dispatch operates on minute-by-minute time scale with 20-40 minutes prediction horizon and responds to any mismatches caused by forecasting error, which is denoted as chance-constrained model predictive control (CCMPC). The CCMPC provides an open-loop schedule for the entire horizon yet only implement the first control decision. This procedure is repeated every minute in receding horizon fashion. The objective of the chance constrained MPC optimization problem is to minimize the deviation of conventional generation from the scheduled set points provided by the economic trajectory.

Contributions of this paper include the following:

- Prior works have explored allocating flexible resources in a techno-economic setting to compute optimal economic trajectories as reference signals for a fast timescale dispatch of energy resources. In this paper, we expand these bilevel frameworks to couple these economic trajectories with a fast timescale stochastic predictive dispatch.
- As far as the authors are aware, prior work on stochastic OPF methods, focuses mainly on the uncertainty of (algebraic) power injections (e.g., wind, demand), which temporally decouples the OPF problem and side-steps the computational challenges of multi-period optimization under uncertainty, e.g., [16], [17]. Unlike those works, this paper presents a stochastic predictive OPF with uncertain dynamic energy capacity and analyze how robustness (i.e., uncertainty in VPP energy capacities) trades off with system performance (i.e., ability of VPP to supply corrective power balancing). Related work in [12], [13], [18] also investigate uncertain energy storage capacity, however, the authors manage that uncertainty through day-ahead reserve scheduling at a 15-60 minute time-scale rather than the stochastic predictive dispatch presented herein.
- Computing optimized charging/discharging commands for uncertain energy resources deterministically, based on the expected energy capacity estimate may result in saturation of the control action under unexpected energy capacity realization. This saturation phenomena gives rise to the notion of dynamic capacity saturation (DCS), which we present and analyze in this paper for the first time. We show that DCS is helpful to describe how uncertain resources can participate in corrective power balancing.

The remainder of this paper is organized as follows. Section II describes the optimal power flow problem and tracking control framework, and discusses the roles of each, and their interactions. In Section III, we explain role of uncertainty on capacity of storage devices and describe chance constrained model predictive control (CCMPC). In Section IV the results of case studies on the modified IEEE 30-bus power system is presented. Finally the concluding remarks and future work are given in Section V.

II. PROBLEM FORMULATION

We consider a transmission system model comprising of N_b buses, N_l lines, N_G generators, N_L loads and N_B VPPs. Given a forecast of demand and expected renewable generation (i.e., net-load) for a number of hours (e.g., day-ahead), an economically optimal trajectory is computed. However, due to

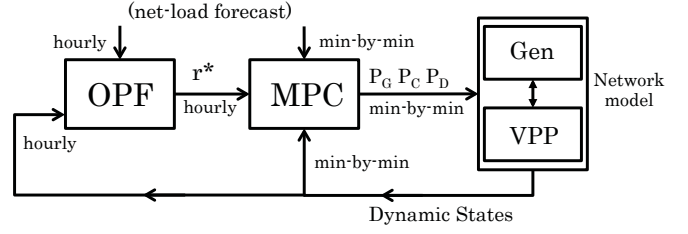


Figure 1. Overview of control scheme showing controller including OPF and MPC part and how each part is related to power grid

forecasting error, it may be necessary for generators to deviate from the predefined trajectory. The controller’s objective is to meet the demand while minimizing the tracking error by utilizing the flexibility of VPPs. This suggests a bi-level control strategy for electric power systems. In this work our focus is on predictive reference tracking-MPC. Figure. 1 provides an overview of the proposed control system.

A. Optimal Economic Trajectory

Like most of related works, e.g., [12], [18], [15], the DC power flow approximation is adopted which gives us a tractable linear representation of the power system while ensuring the convexity of optimization problem.

Based on net-load forecast, the optimal, N_T -hour ahead (i.e. $N_T = 24$), schedule is computed as a multi-period, quadratic programming (QP) problem whose objective is to minimize energy (fuel) costs of conventional generators [19]. Let a [\$/h-pu] and b [\$/h-pu²] are linear and quadratic coefficient of generators cost curve, $P_{G_i} \in \mathbb{R}^{N_G}$ refers to power set point of generator i corresponding to the forecasted load power. With this definition, the resulting objective of the problem can be expressed as:

$$\min_{P_{G_i}} \sum_{\forall k \in N_T} \sum_{\forall i \in N_G} a_i^k P_{G_i}[k] + b_i^k P_{G_i}^2[k], \quad (1)$$

subject to the physical and operational constraints corresponding to the power flow on the system generator and line limits for all $k \in N_T$:

$$P_{Li}^f[k] + \sum_{j \in \Omega_i^N} f_{ij}[k] = \sum_{z \in \Omega_i^G} P_{Gz}[k], \quad (2)$$

$$\underline{P}_{G_i} \leq P_{G_i}[k] \leq \overline{P}_{G_i}, \quad (3)$$

$$-R_{G_i} \leq P_{G_i}[k+1] - P_{G_i}[k] \leq R_{G_i}, \quad (4)$$

$$f_{ij}[k] = b_{ij}(\theta_i[k] - \theta_j[k]), \quad (5)$$

$$\underline{f}_{ij} \leq f_{ij}[k] \leq \overline{f}_{ij}, \quad (6)$$

where Ω_i^N and Ω_i^G refer to set of all buses connected to bus i and set of all generators at bus i . Forecasted electrical net-load (i.e., demand minus renewables) is represented by P_L^f while $\overline{P}_G(P_G^1)$ and R_G represent, maximum (minimum) generation capacity and ramp rate limit of generator, respectively. Also θ_i is the voltage bus angles at bus i and b_{ij} denotes the

¹The lower bounds of the generator set-points would be available from unit commitment (UC) problem which is not within the scope of this paper. In this paper for simplicity the lower bound is assumed to be zero.

imaginary part of the admittance of the line connecting node i to node j and f_{ij} represent power flows on the corresponding line. By solving this problem every hour, a reference signal over a horizon of N_T is established based on the updated measurements and forecasts.

Remark II.1 In this paper, we are assuming that the responsive VPPs are available from previously allocated reserves (e.g., akin to [12]) and have baseline consumption. By shifting the controllable loads consumption from its baseline, VPPs can respond to the instantaneous mismatches caused by forecast error quickly. Any decrease/increase in the consumption of the VPPs relative to its baseline consumption can be translated as discharging/charging the VPPs. That is, we assume that market interactions have determined the regulation capability from each VPP [20].

B. Trajectory tracking and managing uncertainty

Due to mismatches between forecasted and actual values of net-load, forecasted optimal set points of generator may not be a feasible solution for the power flow problem. Therefore, in the second level, a model predictive controller (MPC) is in charge of responding to any deviation in load consumption and renewable production from their predicted value in a way to minimizing the deviation from reference optimal trajectory while satisfying all the constraints such as line limits, generators limit, ramp rate limits of generators and dynamic and power ratings of energy storage devices (VPPs). The MPC iteratively, based on initial states, updated net-load forecast and updated reference signal, optimizing over a finite time horizon, M , by solving an open-loop optimization problem. This yields a sequence of optimal control action for the next M steps, where only applying the first instance of control sequence.

In general, the outcomes of the first level (optimizing under deterministic condition) are used as our base trajectories which already take care of our primal objectives like cost or security while the VPPs make the aggregated flexibility available to controller as balancing reserve and enhance tracking performance. Since time step of MPC (≈ 1 minute) is much shorter than OPF (≈ 1 hour), reference trajectory provided by OPF is interpolated by time step of T_s .

Control actions will be applied for the whole step-width T_s such that $u(t) = u[k]$ for $t \in [kT_s, kT_s + T_s]$. At each time k , the state of the charge (SOC) of VPPs and generator set-points are the dynamic states which are measured and included as initial state of the system for the next step. Based on [15], MPC scheme can be summarized as follows:

- 1) At time k , with initial SOC, S_k , updated net-load forecasts and updated generator set-points from solving OPF, MPC solves a finite-horizon open-loop optimal control problem, over interval $[k, k + M]$. This returns sequence of optimal control action such as charging or discharging VPPs and re-scheduling generator set-points if needed, for the next M steps (k to $k + M$).
- 2) Apply only the control action corresponding to time k
- 3) Measure the actual system state based on the actual load consumption and renewable generation at time $k + 1$.

- 4) Set $k = k + 1$

The open-loop MPC optimization is as follows:

$$J^* = \min_{P_{Gi}, P_{Ci}, P_{Di}} \sum_{m=k}^{k+M} \sum_{\forall i \in N_g} c_G^i (P_{Gi}[m] - P_{Gi}^r[m])^2 \quad (7a)$$

$$+ \sum_{m=k}^{k+M} \sum_{\forall i \in N_B} c_C^i P_{Ci} + c_D^i P_{Di}$$

s.t.

$$P_{Ni}[m] + \sum_{j \in \Omega_i^N} f_{ij}[m] - \sum_{z \in \Omega_i^G} P_{Gz}[m] = 0 \quad (7b)$$

$$P_{Ni}[m] = P_{Ci}[m] - P_{Di}[m] + P_{Li}^f[m] \quad (7c)$$

$$\underline{f}_{ij} \leq f_{ij}[m] \leq \overline{f}_{ij} \quad (7d)$$

$$f_{ij}[m] = b_{ij}(\theta_i[m] - \theta_j[m]) \quad (7e)$$

$$\underline{P_{Gi}} \leq P_{Gi}[m] \leq \overline{P_{Gi}} \quad (7f)$$

$$\underline{P_{Ci}} \leq P_{Ci}[m] \leq \overline{P_{Ci}} \quad (7g)$$

$$\underline{P_{Di}} \leq P_{Di}[m] \leq \overline{P_{Di}} \quad (7h)$$

$$P_{Gi}[m] - P_{Gi}[m-1] \leq R_{Gi} \quad (7i)$$

$$-R_{Gi} \leq P_{Gi}[m-1] - P_{Gi}[m] \leq R_{Gi} \quad (7j)$$

$$S_i[m+1] = S_i[m] + T_s \left(\eta_{ci} P_{Ci}[m] - \frac{1}{\eta_{di}} P_{Di}[m] \right) \quad (7k)$$

$$\underline{S}_i \leq S_i[m] \leq \overline{S}_i \quad (7l)$$

$$S_i[k-1] \leq S_i[k+M] \quad (7m)$$

$$P_{Ci}[m] P_{Di}[m] = 0 \quad (7n)$$

where (7b)-(7l) are satisfied, $\forall m = k, k+1, \dots, k+M$. Note that c_G and c_C (c_D) are positive scalars representing tracking and charging (dis-charging) cost coefficients. Moreover, $P_{Ci}, P_{Di} \in \mathbb{R}_+$ are positive scalars representing charging and discharging commands of VPPs and P_{Gi}^r is the reference signal. $\overline{P_{Ci}}$ ($\overline{P_{Di}}$) and \overline{S}_i represent the maximum charging (discharging) power capacity and the maximum energy capacity of VPP located at bus i , respectively. Similarly, $\underline{P_{Ci}}$ ($\underline{P_{Di}}$) and \underline{S}_i represent the minimum charging (discharging) power rate and the minimum energy level of the VPPs which in our work assumed to be equal to zero for simplicity. The charging and discharging efficiency of VPP located at bus i are denoted η_{ci} and η_{di} respectively. The net power injected from VPP i at time m equal to $(P_{Ci}[m] - P_{Di}[m])$ that could be positive (charging the VPP) or negative (discharging) or zero. We impose terminal constraint (7m) on SOC of VPPs to ensure sustainability of VPP resources at the end of each optimization horizon.

Remark II.2 To prevent simultaneous charging and discharging which is not physically realizable for most of the storage devices, complementary condition (7n) is employed, however since this constraint is non-linear, it makes the problem strongly non-convex and needs applying mixed-integer approach [21]. Authors in [14] employed a heuristic method that enabled them to solve the convex problem while preventing simultaneous charging and discharging. Furthermore, as VPPs aggregate large population of small-scale flexible energy resources, they have the ability to send charging and discharging commands to different devices in their group simultaneously and the aggregated charging and discharging commands are what determine the next time steps overall energy level.

III. THE CHANCE CONSTRAINED PROBLEM

VPPs can be formed from a large number of different resources including storage devices, wind farms, solar farms as well as different forms of flexible energy resources like plug-in electric vehicles (EVs) and TCLs [22]. The flexibility offered by VPPs can enable renewable integration into the power system and provide significant balancing reserves to the system operator and prevent frequent rescheduling due to imbalances from weather and load/demand forecasts. However, the level of the flexibility that VPPs can provide to system operator is uncertain itself. As an example, coordinated aggregation of large population of TCLs is often modeled as virtual storage resources [23]. However, due to stochastic and time-varying human usage of hot-water, the size of the virtual storage resources is time-varying. More specifically, available flexibility offered by aggregated TCL to the system operator, which can be translated to the upper bound of the virtual storage resource, is a function of different stochastic quantities such as weather condition and human behavior. Flexibility offered by each device is uncertain and considered an independent random variable (i.e. background usage of other devices). Since, VPPs are formed from a large number of flexible resources, the central limit theorem implies that the VPP's energy capacity is a normally distributed random variable centered on the true mean (i.e. $\bar{S} \sim \mathcal{N}(\mu, \sigma^2)$). Thus, the stochastic variable (\bar{S}) is present only on the right hand side of (71).

Definition III.1 Dynamic capacity saturation (DCS): Computing optimized control actions, such as charging/discharging commands, for uncertain energy resources that provide balancing reserves can be based on a mean (or average) energy capacity estimate. When using the mean capacity values result in a deterministic optimization problem. However, the underlying uncertain energy capacity may realize itself unexpectedly and saturate (or zero out) the optimized control action. We call this saturation phenomenon *dynamic capacity saturation (DCS)*. Under DCS, an energy resource may saturate, which zeros out its control action, leading to unexpected power imbalances in the system. To regulate these DCS-induced imbalances, grid operators must rely on (expensive) generation to supply the difference based on their participation factor d_i , as shown in (8). In addition, SOC of VPP could be updated to reflect actual capacity as shown in (9). Figure 2 shows an example of how forecast errors lead to DCS. Plot (a) illustrates the expected and actual capacity of VPP (dotted lines). Also, the state evolution of SOC based on the expected capacity of VPP and needed correction due to forecasting error are shown (dashed lines). Plot (b) and (c) show the optimal schedule for charging/discharging of VPP and how DCS causes deviation from optimal solution:

$$\Delta P_{Gi}[k+1] = -d_i \sum_{i \in N_b} T_s^{-1} \max(S_i[k+1] - \bar{S}_i, 0) \quad (8)$$

$$S_i[k+1] = \max(S_i[k+1], \bar{S}) \quad (9)$$

Since the capacity of VPP is a stochastic variable, we could approach the problem in a probabilistic manner. The

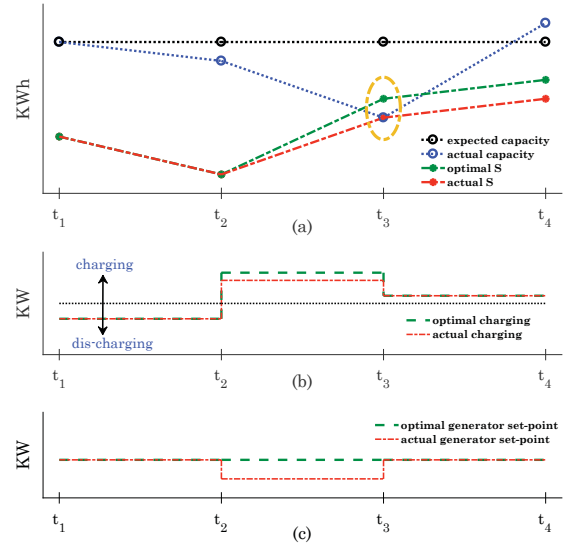


Figure 2. An example of how forecast error causes dynamic capacity saturation.

chance constraint is one such option whereby we decide on the probability level of $1 - \epsilon$, where $\epsilon \in (0, 1)$, as shown below

$$\mathbb{P}(S_i[k+1] \leq \bar{S}_i(\delta)) \geq 1 - \epsilon \quad (10)$$

In [10], a scenario is introduced, in which the chance constraint is substituted by a finite number of deterministic constraints and provide a-priori guarantees on satisfying the chance constraint with some certain level of confidence β , where $\beta \in (0, 1)$. Ref. [9] proposed a two step method based on [10] that results in a lower number of realizations. In the first step, the set Δ , including at least $1 - \epsilon$ probability mass of uncertainty, is made with confidence level of at least $1 - \beta$. To form this set, we need at least N realizations, where e denotes the Euler number and N is calculated based on the number of uncertain parameters N_ω ,

$$N \geq \frac{1}{\epsilon} \frac{e}{e-1} (\ln \frac{1}{\beta} + 2N_\omega - 1) \quad (11)$$

Based on the set Δ , the chance constraint is substituted to the robust constrain

$$S_i[k+1] \leq \bar{S}_i(\delta) \quad \text{for all } \delta \in \Delta \quad (12)$$

While only expected value of capacity of VPP is needed to come up with a deterministic solution, N realizations are needed for a probabilistic solution. For example, to ensure a violation probability of maximum $\epsilon = 0.1$ with a confidence level of $\beta = 0.05$, in presence of one VPP with uncertain capacity, we need to consider 64 realizations of VPP capacity as shown in Fig 3. The green, dashed line represents expected values and the red, solid line represent the robust bound.

We introduce coefficient $\alpha \in [0, \text{inf}]$, as an average level of robustness to investigate role of robustness on performance of the controller.

$$\bar{S} = \alpha \bar{S}_{\text{expected}} \quad (13)$$

By setting α based on the robust bound (e.g, robust bound computed by scenario approach), we can reduce the probability of DCS, but part of the flexibility offered by VPPs will

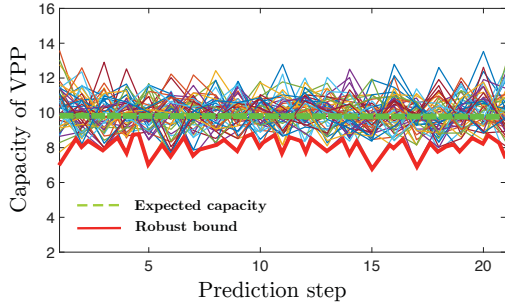


Figure 3. Expected value of VPP capacity versus 64 realizations

be dismissed. On the other hand, by selecting $\alpha \geq 1$, the predictive optimizer will have more VPP resources available for balancing, however, DCS will occur more frequently in the system, which can reduce closed-loop performance (i.e., generator having to make up the slack resulting from DCS.) Therefore, there should be a balance between robustness and flexibility. i.e. coefficient α must be chosen in such a way that controller can use the most flexibility offered by VPPs and minimize chances of DCS².

IV. SIMULATION RESULT

In this section, the introduced control approach is applied to modified IEEE 30 bus power system [24]. The power system is modified to include one VPP at bus 5. All optimization problem were solved via the MATLAB and AMPL using the solver GUROBI.

A. Perfect prediction of VPP capacity

Initially, we assume that the capacity of VPP can be forecasted perfectly. Based on the forecasts of net-load, an optimal schedule for generators is computed. To model net-load forecast error raised from uncertain renewable generation, mean reverting random walk with zero mean is added to the forecasted net-load. Performance and behavior of MPC (with horizon length of $M = 20$) is shown in Fig. 4. Recall that reference signal is the generator set-point, which means high performance implies generators do not respond to imbalances (i.e., do not ramp through reserves). Obviously, in presence of VPP, tracking performance is improved and the flexibility offered by VPP, make MPC able to effectively limit the ramping up or down of generators. However, the tracking error can not be zero due to limited capacity of VPP.

TABLE I
RUN-TIME METRICS FOR OPF AND MPC

	Average (s)	Standard deviation (s)
OPF (hourly)	0.5045	0.0021
MPC ($M = 40$ mins)	1.8289	0.0035

²The forecasting error occurs almost at all time steps (e.g., see Fig 2a for $t > t_1$). However, despite forecast errors, sub-optimal solution happens only when DCS occurs (e.g., see Fig 2a at $t = t_3$). If DCS is absent, optimal regulation can be achieved despite forecasting errors.

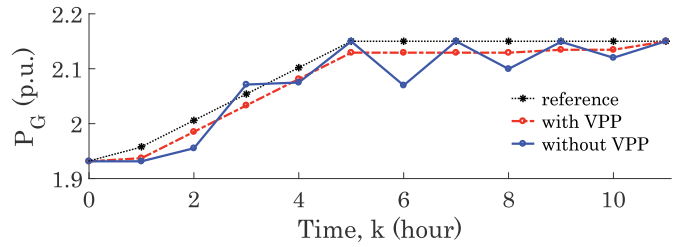


Figure 4. Optimal schedule based on the forecasted net-load as a reference trajectory and performance of the MPC scheme for one generator under two cases: without VPP and with VPP.

B. Uncertain VPP capacity

In this part, we assumed that the expected capacity of VPP is given and the probability distribution of the uncertainty is known. The actual capacity of VPP at each time step is computed as

$$\bar{S}_{\text{act}} = (1 + \zeta/10)\bar{S}_{\text{expected}}, \quad (14)$$

where ζ is normally distributed (i.e. $\zeta \sim \mathcal{N}(0, 1)$).

To investigate the role of uncertain capacity of VPP in tracking performance of MPC, a simple forecast of net-load that stays constant over the next 24 hours is created. Actual net-load is created by injecting 20 percent step down and 10 percent step up error while each error persists for 10 minutes, as shown in Fig 5. A comparison of the tracking performance of deterministic and robust approaches, at $\alpha = 0.9$, is provided in Fig. 6.

The first plot shows one realization of actual capacity of VPP, \bar{S} (dashed blue line) and state evolution of SOC of VPP under the deterministic and robust approaches. The second plot shows optimal schedule for charging/discharging VPP under the deterministic and robust approaches. And the third plot shows tracking performance of the system under different scenarios. As illustrated, under deterministic approach, DCS occurs twice (i.e. before and after $t = 30$ in the first plot) which cause unscheduled adjustment in generator power (red dashed line in the third plot). Although by using robust approach part of the offered flexibility is dismissed, chance of DCS reduces which leads to less generators adjustment.

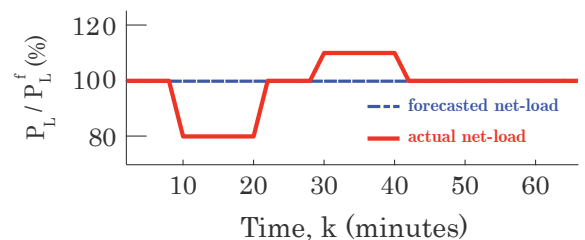


Figure 5. The actual net-load is created by injecting 10 minutes long, step down and step up error to the forecasted net-load.

To evaluate the tracking performance of deterministic and robust approaches under stochastic behavior of VPP capacity, 100,000 repeated trials are performed. Each trial differs in expected capacity of VPP (0.4 p.u. and 0.8 p.u.) and α (from 0 to 2). Objective functions of robust approach J_R^* and deterministic approach J_D^* are used as a metric for the tracking

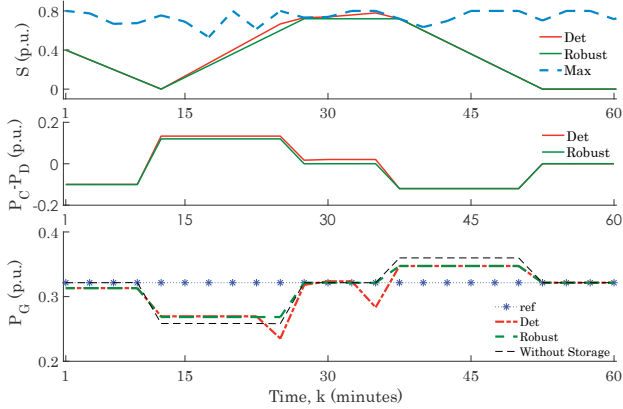


Figure 6. The tracking performance of system under three different scenarios: no VPP, deterministic approach and robust approach.

performance. Smaller objective means less average deviation from scheduled set-points and indicates better tracking. Figure 7 shows J_R^* , J_D^* and their ratio, at $\alpha = 0.9$, where capacity of VPP is 0.8 p.u. for 2000 trials. The results of deterministic and robust approaches where capacity of VPP equals 0.4 p.u. and 0.8 p.u., at $\alpha = 0.9$, is shown in Table II.

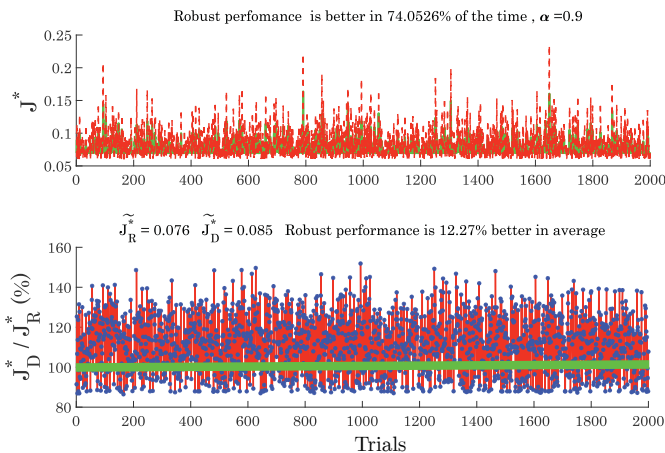


Figure 7. The first plot compares J_D^* and J_R^* for 2000 trials (VPP capacity = 0.8 pu) and the second plot illustrates their ratio. Any points above the green line indicates better performance of the robust approach. The robust approach outperformed the deterministic approach on 1480 of the 2000 trials and on average, it is 12% better.

TABLE II
COMPARING THE AVERAGE OF J_D^* , J_R^* AND THEIR RATIO AS A METRIC OF PERFORMANCE BASED ON 2000 TRIALS

$E(\bar{S})$	\bar{J}_D^*	\bar{J}_R^*	\bar{J}_D^*/\bar{J}_R^*	$J_D^* > J_R^*$
0.4 p.u.	0.1390	0.1336	1.0402	83%
0.8 p.u.	0.0848	0.0756	1.1227	74.5%

Figure 8 compares the average tracking performance under deterministic and robust approach for different values of α (i.e. level of robustness). By choosing a small α (conservative choice), DCS occurs less frequently, however, larger part of flexible resources are not utilized. By choosing large α , the

controller benefits from the full flexibility offered by resource. However, by discounting the role of uncertainty, DCS occurs more frequently and consequently generators rescheduling is needed more often. In both of these cases, the deterministic approach outperforms the robust one (i.e. $J_D^* < J_R^*$). If α is chosen appropriately, the flexibility offered by the VPPs can be used effectively while limiting occurrence of DCS. In other words, sacrificing some robustness in dispatching the uncertain resource leads to improved tracking performance. It is interesting to note that in the scenario-based approach with typical selection of $\epsilon = 0.1$ and $\beta = 0.05$, 64 realizations are needed based on (11) and we would get an equivalent $\alpha = 0.75$, for which the deterministic (average) approach actually outperforms the robust approach (i.e., it is overly conservative). However, equivalent violation probability of $\alpha = 0.85$ in which the robust approach (on average) outperforms the deterministic one by 4.5% is a non-intuitive $\epsilon = 0.6$.

To explore the performance of the robust approach for a more general net-load scenarios, a mean reverting random walk (MRRW) noise is added to the actual load profile shown in Fig. 5, and 1000 realizations are created (Fig. 9). Table III provides result of the tracking performance of robust and deterministic approaches regarding the 1000 trials. To better understand the effect of DCS on performance of the controller, the total number of times that DCS occurs N^{DCS} using each method is calculated. Note that each trial includes 60 time-steps (minutes) and 1000 trials are considered for each scenario of capacity of VPP. Therefore, N^{DCS} is computed with respect to 60000 time-steps.

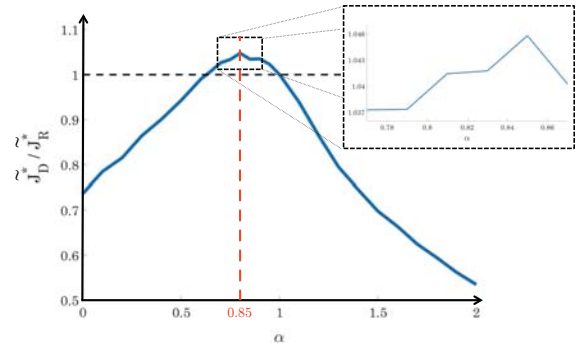


Figure 8. Trade-off between robustness and tracking performance (VPP capacity = 0.4 pu). Average ratio of J_D^* and J_R^* is used as a metric for performance of the system regarding to the different levels of the robustness. At $\alpha = 0.85$, on average the robust approach is 4.5% better than the deterministic one.

TABLE III
COMPARING AVERAGE PERFORMANCE OF THE SYSTEM UNDER DETERMINISTIC AND ROBUST APPROACH WITH 1000 TRIALS

$E(\bar{S})$	\bar{J}_D^*	\bar{J}_R^*	\bar{J}_D^*/\bar{J}_R^*	$J_D^* > J_R^*$	N_D^{DCS}	N_R^{DCS}
0.4 p.u.	0.1536	0.1480	1.0376	83%	2867	1769
0.8 p.u.	0.0947	0.0884	1.0713	69%	2089	1045

V. CONCLUSION AND FUTURE WORK

This paper studies the performance of a bilevel receding-horizon predictive optimal power flow problem for managing

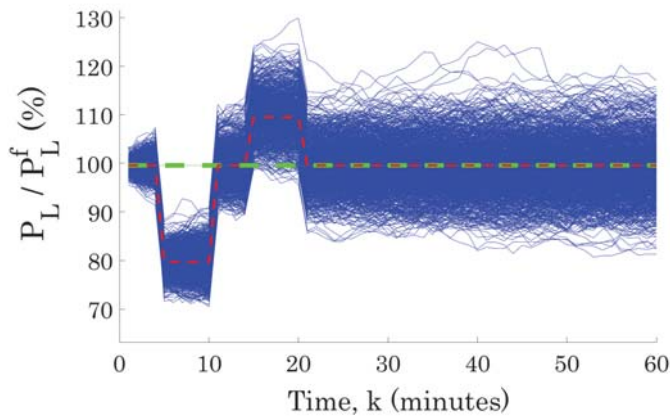


Figure 9. One thousands realization of load profiles are created based on the Fig. 5 while the green dashed line shows the forecasted load and the red line shows mean of all created load profiles.

short-term variability with grid assets (VPPs) that are uncertain in their energy capacity. This gives rise to the notion of dynamic capacity saturation (DCS) for uncertain energy resources. The numerical studies indicate that there exists a sensitive trade-off between robustness of the optimized dispatch (i.e., severity of DCS) and closed-loop system performance (i.e., VPPs ability to provide regulating reserves). It is shown that sacrificing some robustness in the dispatch of the uncertain energy capacity can significantly improve system performance (up to 4-12%). Interestingly, the popular approach of robustifying chance-constraints with scenario-based sampling may lead to reduced closed-loop system performance. Future work will focus on analytically quantifying the effects of DCS on the closed-loop response and developing tools that optimally manages storage commitment under dynamic uncertainty (i.e., α). Additionally, we plan to extend the current work to consider multi-VPPs with uncertain capacity under system constraints such as line flow limits, and address the question of where the VPPs should be placed and how many VPPs are advantageous for a given power network.

REFERENCES

- [1] G. Strbac, "Demand side management: Benefits and challenges," *Energy policy*, vol. 36, no. 12, pp. 4419–4426, 2008.
- [2] M. Arnold and G. Andersson, "Model predictive control of energy storage including uncertain forecasts," in *Power Systems Computation Conference (PSCC), Stockholm, Sweden*, vol. 23, 2011, pp. 24–29.
- [3] D. S. Callaway and I. A. Hiskens, "Achieving controllability of electric loads," *Proceedings of the IEEE*, vol. 99, no. 1, pp. 184–199, 2011.
- [4] S. P. Meyn, P. Barooah, A. Bušić, Y. Chen, and J. Ehren, "Ancillary service to the grid using intelligent deferrable loads," *IEEE Transactions on Automatic Control*, vol. 60, no. 11, pp. 2847–2862, 2015.
- [5] M. Amini and M. Almassalkhi, "Investigating delays in frequency-dependent load control," in *2016 IEEE Innovative Smart Grid Technologies - Asia (ISGT-Asia)*, Nov 2016, pp. 448–453.
- [6] M. Almassalkhi, J. Frolik, and P. Hines, "Packetized energy management: Asynchronous and anonymous coordination of thermostatically controlled loads," in *2017 American Control Conference (ACC)*, May 2017, pp. 1431–1437.
- [7] M. Almassalkhi, Y. Dvorkin, J. Marley, R. Fernández-Blanco, I. Hiskens, D. Kirschen, J. Martin, H. Pandžić, T. Qiu, M. Sarker *et al.*, "Incorporating storage as a flexible transmission asset in power system operation procedure," in *Power Systems Computation Conference (PSCC)*, 2016. IEEE, 2016, pp. 1–7.
- [8] J. L. Mathieu, M. G. Vay, and G. Andersson, "Uncertainty in the flexibility of aggregations of demand response resources," in *IECON 2013 - 39th Annual Conference of the IEEE Industrial Electronics Society*, Nov 2013, pp. 8052–8057.
- [9] K. Margellos, P. Goulart, and J. Lygeros, "On the road between robust optimization and the scenario approach for chance constrained optimization problems," *IEEE Transactions on Automatic Control*, vol. 59, no. 8, pp. 2258–2263, 2014.
- [10] G. C. Calafiore and M. C. Campi, "The scenario approach to robust control design," *IEEE Transactions on Automatic Control*, vol. 51, no. 5, pp. 742–753, 2006.
- [11] X. Zhang, K. Margellos, P. Goulart, and J. Lygeros, "Stochastic model predictive control using a combination of randomized and robust optimization," in *52nd IEEE Conference on Decision and Control*, Dec 2013, pp. 7740–7745.
- [12] M. Vrakopoulou, B. Li, and J. L. Mathieu, "Chance constrained reserve scheduling using uncertain controllable loads Part I: Formulation and scenario-based analysis," *IEEE Transactions on Smart Grid*, 2017.
- [13] B. Li, M. Vrakopoulou, and J. L. Mathieu, "Chance constrained reserve scheduling using uncertain controllable loads Part II: Analytical reformulation," *IEEE Transactions on Smart Grid*, vol. PP, no. 99, pp. 1–1, 2017.
- [14] M. R. Almassalkhi and I. A. Hiskens, "Model-predictive cascade mitigation in electric power systems with storage and renewables-Part I: Theory and implementation," *IEEE Transactions on Power Systems*, vol. 30, no. 1, pp. 67–77, 2015.
- [15] —, "Model-predictive cascade mitigation in electric power systems with storage and renewables-Part II: Case-study," *IEEE Transactions on Power Systems*, vol. 30, no. 1, pp. 78–87, 2015.
- [16] B. Li, S. D. Maroukis, Y. Lin, and J. L. Mathieu, "Impact of uncertainty from load-based reserves and renewables on dispatch costs and emissions," in *2016 North American Power Symposium (NAPS)*, Sept 2016, pp. 1–6.
- [17] Y. Zhang and J. L. Mathieu, "Two-stage Distributionally Robust Optimal Power Flow with Flexible Loads," *PowerTech*, 2017.
- [18] K. Baker, G. Hug, and X. Li, "Energy storage sizing taking into account forecast uncertainties and receding horizon operation," *IEEE Transactions on Sustainable Energy*, vol. 8, no. 1, pp. 331–340, Jan 2017.
- [19] A. J. Wood and B. F. Wollenberg, *Power generation, operation, and control*. John Wiley & Sons, 2012.
- [20] B. Henson. Regulation performance monitor. [Online]. Available: https://www.iso-ne.com/static-assets/documents/support/training/courses/energy_mkt_ancil_serv_top/regulation_performanc_monitor_rollout.pdf
- [21] L. Bai, J. E. Mitchell, and J.-S. Pang, "On convex quadratic programs with linear complementarity constraints," *Computational Optimization and Applications*, vol. 54, no. 3, pp. 517–554, 2013.
- [22] S. M. Nosratabadi, R.-A. Hooshmand, and E. Gholipour, "A comprehensive review on microgrid and virtual power plant concepts employed for distributed energy resources scheduling in power systems," *Renewable and Sustainable Energy Reviews*, vol. 67, no. Supplement C, pp. 341–363, 2017.
- [23] M. Almassalkhi, J. Frolik, and P. Hines, "Packetized energy management: asynchronous and anonymous coordination of thermostatically controlled loads," in *American Control Conference (ACC)*, 2017. IEEE, 2017, pp. 1431–1437.
- [24] R. D. Zimmerman, C. E. Murillo-Sanchez, and R. J. Thomas, "Matpower: Steady-state operations, planning, and analysis tools for power systems research and education," *IEEE Transactions on Power Systems*, vol. 26, no. 1, pp. 12–19, Feb 2011.